Available online at www.sciencedirect.com
SCIENCE DIRECT®
Hearing Research 196 (2004) 94–108
HEARING RESEARCH
www.elsevier.com/locate/heares

Temporary DPOAE level shifts, ABR threshold shifts and histopathological damage following below-critical-level noise exposures

Gary W. Harding *, Barbara A. Bohne

Department of Otolaryngology, Washington University School of Medicine, P.O. Box 8115, 660 South Euclid, St. Louis, MO 63110, USA

Received 22 January 2004; accepted 8 March 2004
Available online 18 August 2004

Abstract

DPOAE temporary level shift (TLS) at $2f_1-f_2$ and f_2-f_1, ABR temporary threshold shift (TTS), and detailed histopathological findings were compared in three groups of chinchillas that were exposed for 24 h to an octave band of noise (OBN) centered at 4 kHz with a sound pressure level (SPL) of 80, 86 or 92 dB ($n=3,4,6$). DPOAE levels at 39 frequencies from $f_1=0.3$ to 16 kHz ($f_2/f_1=1.23$; L_2 and $L_1=55$, 65 and 75 dB, equal and differing by 10 dB) and ABR thresholds at 13 frequencies from 0.5 to 20 kHz were collected pre- and immediately post-exposure. The functional data were converted to pre- minus post-exposure shift and overlaid upon the cytocochleogram of cochlear damage using the frequency-place map for the chinchilla. The magnitude and frequency place of components in the $2f_1-f_2$ TLS patterns were determined and group averages for each OBN SPL and L_1, L_2 combination were calculated. The f_2-f_1 TLS was also examined in ears with focal lesions equal to or greater than 0.4 mm. The $2f_1-f_2$ TLS (plotted at f_1) and TTS aligned with the extent and location of damaged supporting cells. The TLS patterns over frequency had two features which were unexpected: (1) a peak at about a half octave above the center of the OBN with a valley just above and below it and (2) a peak (often showing enhancement) at the apical boundary of the supporting-cell damage. The magnitudes of the TLS and TTS generally increased with increasing SPL of the exposure. The peaks of the TLS and TTS, as well as the peaks and valleys of the TLS pattern moved apically as the SPL of the OBN was increased. However, there was little consistency in the pattern relations with differing L_1, L_2 combinations. In addition, neither the $2f_1-f_2$ nor f_2-f_1 TLS for any L_1, L_2 combination reliably detected focal lesions (100% OHC loss) from 0.4 to 1.2 mm in size. Often, the TLS went in the opposite direction from what would be expected at focal lesions. Recovery from TLS and TTS was also examined in seven animals. Both TLS and TTS recovered partially or completely, the magnitude depending upon exposure SPL.

Keywords: DPOAE; ABR; Noise; Organ of Corti; Histopathology; Chinchilla

1. Introduction

Distortion product otoacoustic emissions (DPOAE) are presumed to be produced by the summed activity of outer hair cells (OHC) (e.g., Chang and Norton, 1996). Auditory brainstem responses (ABR) appear to be dominated by the activity of inner hair cells (IHC). The magnitude and extent of permanent ABR threshold shifts correlate well with IHC and nerve fiber

* Corresponding author. Tel./fax: +1-314-362-7497.
E-mail address: hardingg@wustl.edu (G.W. Harding).

Abbreviations: ABR, auditory brainstem response; DPOAE, distortion product otoacoustic emission; IHC, inner hair cell; OBN, octave band of noise; OC, organ of Corti; OHC, outer hair cell; SPL, sound pressure level; TLS, temporary level shift; TTS, temporary threshold shift

0378-5955/$ - see front matter © 2004 Elsevier B.V. All rights reserved.
doi:10.1016/j.heares.2004.03.011

loss (e.g., Nordmann et al., 2000). It has been tacitly assumed that anything which produces a functional deficit in or complete loss of a substantial number of OHCs would have a profound effect upon DPOAEs. In some instances, when the cochleae were examined histopathologically, this assumption was mostly confirmed (e.g., Canlon and Fransson, 1995; Martin et al., 2002). However, in other studies in which correlations were made between OHC loss and DPOAEs, this assumption was not supported (e.g., Harding et al., 2002; Avan et al., 2003).

In a previous report (Harding et al., 2002), we examined the frequency-place alignment of noise-induced DPOAE level shifts and ABR threshold shifts (pre-minus post-exposure) with a detailed assessment of the histopathological damage from a high-level, short-duration noise exposure (4 kHz OBN, 108 dB SPL, 1.75 h). It was found that: (1) the best correlation of DPOAE level shifts with the noise-induced hair-cell loss required plotting these data at f_1; (2) level shifts reflected different correlates for temporary and permanent hearing loss (i.e., supporting-cell damage leading to stereocilia uncoupling versus hair-cell loss); (3) level shifts did not detect relatively large focal lesions (i.e., >0.6 mm, 100% OHC loss) and (4) partial recovery of level shifts occurred in regions of complete organ of Corti (OC) loss (i.e., OC wipeout).

Subsequently, it was found that in these cochleae, there were discontinuities in the reticular lamina (Ahmad et al., 2002) and that these lesions appear to be a consequence of above-critical-level exposures (i.e., SPL above which there is no relation between total exposure energy and hearing or hair-cell loss; Harding and Bohne, 2004). In the present report, we examined the changes in DPOAE levels and ABR thresholds with below-critical-level, longer duration noise exposures (i.e., SPLs at which there is a clear relation between total exposure energy and hair-cell loss), particularly as they relate to the effects immediately post-exposure. We hypothesized that by removing the secondary effects of high-level noise exposures (i.e., those occurring post-exposure), DPOAE level shifts would more clearly reflect underlying primary effects (i.e., those occurring during the exposure; Bohne and Harding, 2000).

2. Materials and methods

2.1. Animals

Thirteen 1 to 2-year-old chinchillas were used in the study. The animals were anesthetized during DPOAE levels and ABR thresholds testing with a mixture of ketamine (40 mg/ml), acepromazine (1 mg/ml) and atropine (0.04 mg/ml), given at a dosage of 1 ml/kg body weight. Supplemental anesthetic doses (0.33 ml/kg) were administered as needed during ABR testing. First, ABR thresholds were determined in both ears, followed by collection of DPOAE levels in both ears while the anesthesia level was a little lighter. Baseline DPOAE levels and ABR thresholds were determined one day pre-noise-exposure using the same methods described below for functional testing post-exposure. The protocol for animal use was approved by Washington University's Animal Studies Committee (#20000131 and 20030093; Adverse Effects of Noise on Hearing: Basic Mechanisms; B.A. Bohne, PI).

2.2. Noise exposure

The animals were exposed awake while individually housed in a cage suspended in the middle of a reverberant, soundproof booth. The exposure was an octave band of noise (OBN) with a center frequency of 4 kHz and a sound pressure level (SPL) of 80 ($n=3$), 86 ($n=4$) or 92 ($n=6$) dB for 24 h. A Brüel and Kjaer 2203 sound level meter with a 12.7-mm microphone was used to calibrate sound pressure ±1 dB. Some of the data from the group of animals exposed at 80 dB SPL were reported previously (Harding et al., 2002). Further analysis of the results from these animals is presented here.

2.3. Functional testing

DPOAEs were recorded at 39 frequencies from $f_1=0.3$ to 16 kHz and ABR thresholds at 13 frequencies from 0.5 to 20 kHz. DPOAEs were elicited with tones produced by a pair of Etymotic ER-2 insert earphones and recorded with an Etymotic ER-10B+ microphone. ABRs were elicited with clicks and tone pips using the same ER-2 earphones. DPOAE levels were collected at equal and unequal input levels (L_1 and L_2) ranging from 75 down to 55 dB in 10 dB steps. The combinations used in each animal are shown in Table 1. For the noise exposures used, $2f_1-f_2$ DPOAE magnitudes dropped into the noise floor in the region of maximal shift when L_1 or L_2 was below 55 dB (data not shown). The frequency ratio (f_2/f_1) was 1.23 (see Harding et al., 2002 for recording details). DPOAE levels and ABR thresholds were determined in both ears immediately post-exposure in all animals. Six animals were sacrificed shortly after testing to correlate DPOAE temporary level shift (TLS) and ABR temporary threshold shift (TTS) with the pattern of cochlear injury and degeneration. Seven animals were allowed to recover a variable length of time (i.e., 6–24 days) before their cochleae were fixed for histopathological examination. Functional testing in these latter animals was performed several times during the recovery period, the number depending upon recovery duration.

Table 1
Animals, exposure SPLs, and L_1, L_2 combinations used in the present study

Animal	SPL(dB)	L_1, L_2 (dB)					
		75, 75	75, 65	75, 55	65, 65	65, 55	55, 55
963	80	x	x[a]		x	x[a]	x
964	80	x	x[a]		x	x[a]	x
965	80	x			x		x
	Total ears	6	4	0	6	4	6
960[b]	86	x					
967	86		x		x	x	x
974	86		x		x	x	x
975	86		x		x	x	x
	Total ears	2	6	0	6	6	6
985	92		x		x	x	x
986	92		x		x	x	x
987	92		x	x	x	x	x
988	92		x	x	x	x	x
989	92		x[c]	x[c]	x[c]	x[c]	x[c]
991	92		x	x	x	x	x
	Total ears	0	11	7	11	11	11

[a] $L_1 = L_2 - 10$ dB.
[b] Recorded at slightly different frequencies from the others.
[c] 989-Right not included due to poor pattern correlations with the others in this group.

2.4. Tissue processing

Under deep anesthesia, the cochleae were fixed in vivo by perfusing a solution of 1% osmium tetroxide in Dalton's buffer through the perilymphatic scalae for 5 min. After both cochleae were fixed, they were separated from the skull and immersed in a large volume of cold fixative for 2 h. After fixation, the cochleae were washed in Hank's balanced salt solution (three 15-min changes) then placed in 70% ethanol and refrigerated overnight. The following day, the cochleae were dehydrated in a graded series of ethanol followed by propylene oxide, infiltrated with Durcupan then embedded in the same medium (see Bohne and Harding, 1993 for details). After polymerization for 48 h, the cochleae were dissected into flat preparations that were analyzed for hair-cell loss and other histopathological changes by phase-contrast microscopy at magnifications of 625 and 1250×.

2.5. Quantitative and qualitative histopathological analysis

Organ-of-Corti length was measured and missing IHC, OHC, and inner and outer pillar cells were counted from apex to base. The percentage of missing nerve fibers was estimated (see Bohne et al., 1990 for details). The apex-to-base extent of buckled pillar cells and partly collapsed Deiters' cells were determined qualitatively. A cytocochleogram was prepared for each cochlea to present these data relative to the percentage distance from the OC apex.

2.6. Data processing

DPOAE level shifts and ABR threshold shifts were calculated by subtracting post-exposure from pre-exposure magnitudes. The differential noise floor (i.e., the maximum measurable shift) was determined by subtracting post-exposure noise floor magnitudes from pre-exposure DPOAE magnitudes. The distortion product, $2f_1 - f_2$, was the focus of this analysis and comparison with cochlear damage. However, the results from $f_2 - f_1$ distortion products were also examined in part. The $2f_1 - f_2$ DPOAE level shift and ABR threshold shift results were overlaid upon the cytocochleograms using the frequency-place map for the chinchilla (Eldredge et al., 1981) to align the functional changes on the cytocochleogram. The logarithmic mean was used to calculate the mean of DPOAE TLS and ABR TTS across animals. The harmonic mean was used to calculate the mean frequencies at which components in the responses occurred.

3. Results

3.1. Temporary level shift

An example of the correlation among TLS, TTS and histopathology is shown in Fig. 1. OHC loss (solid line on the cytocochleogram, Fig. 1(a)) was minimal across frequency except for a 1-mm region from 4 to 6 kHz with 100% loss. IHC loss (short-dashed lines on cytocochleogram, Fig. 1(a)) was minimal throughout the cochlea. OHCs in the third row were misshapen from 1.5 to 4 kHz and 6 to 10 kHz. The supporting cells, especially the pillars, were buckled from 1 to 8 kHz (horizontal bars in OC box, Fig. 1(a)). Reisner's membrane had been displaced toward the reticular lamina over 1 to 20 kHz from its normal position and the endolymphatic space was reduced (lower horizontal bar in ES box). This pathology was visible in the dissection microscope when the OC segments were viewed at a radial angle. Viewed by light microscopy at 1250×, the stria vascularis contained vacuoles from its apical tip to 0.3 kHz (upper horizontal bar in ES box). Among the ears in the present study, these latter two pathologies were seen only in this ear and were thought to have been present before the noise exposure.

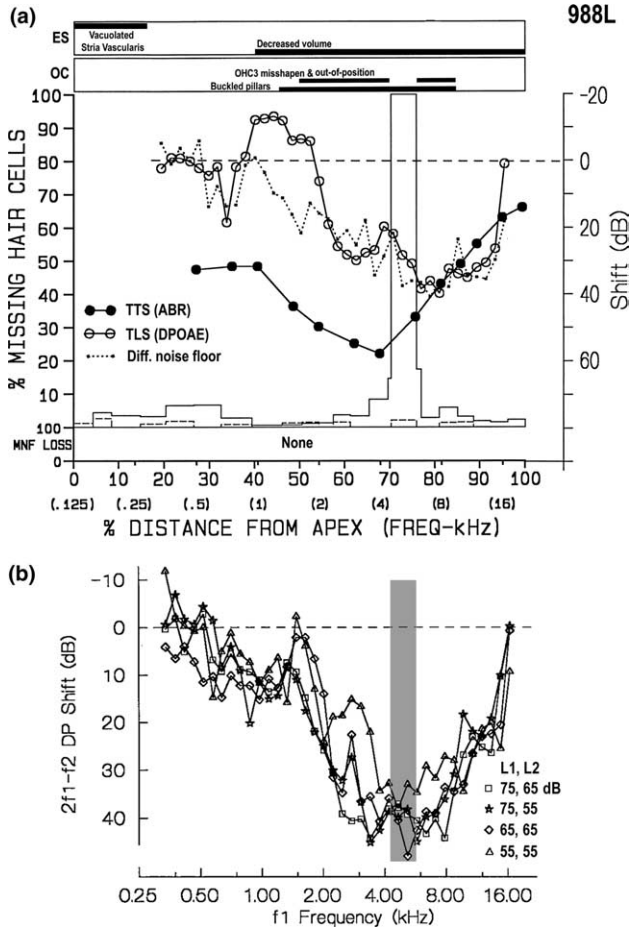

Fig. 1. (a) Cytocochleogram and functional data from cochlea 988L (exposed at 92 dB SPL). Percent (left y-axis) OHC loss (solid line) and IHC loss (short dashed line) as a function of percent distance (frequency place in kHz) from the OC apex (x-axis). The magnitude of TLS (open circles; plotted at f_1), differential noise floor (dotted line), and TTS (filled circles) are overlaid (right y-axis). OHC focal lesion (100% loss) from 4 to 6 kHz. Qualitative histopathology results (top) and nerve fiber loss (bottom). Pillar cells were buckled from 1 to 8 kHz (OC box; lower horizontal bar) and third row OHCs were misshapen and out-of-position from 1.5 to 8 kHz (OC box; upper horizontal bars). Endolymphatic space was decreased from normal (ES box; lower horizontal bar) and the stria vascularis was vacuolated (ES box; upper horizontal bar). There was no nerve fiber loss (MNF LOSS box). (b) TLS for L_1, L_2 combinations not shown in (a) (L_1, L_2 = 75, 65, squares; 75, 55, stars; 65, 65, diamonds; 55, 55, triangles). Region of focal lesion in A is indicated by vertical gray bar. Error bars omitted for clarity. TLS y scales in (a) and (b) differ.

The immediate post-exposure TLS at L_1, L_2 = 65, 55 dB (open circles) and the TTS (solid circles) are overlaid upon the cytocochleogram. These data are plotted at f_1 because this alignment produced the best agreement between noise-induced DPOAE level shifts and hair-cell loss (see also Harding et al., 2002). The level shift curves would move exactly two points to the right if the data were aligned at f_2.

The TLS was maximal (~40 dB) at about 8 kHz and had a local valley (~30 dB) at about 3 kHz with an intervening local peak (~20 dB) at 4 kHz. These two local valleys were at the noise floor. There was a negative peak (~−10 dB) centered at about 1 kHz with a leading local valley (~20 dB) in the noise floor. The maximal TTS (58 dB) occurred at 4 kHz (see also another example of this frequency-specific pattern in Fig. 3). The TTS at 0.5–1 kHz was unusually large which was probably due to the vacuolated stria vascularis which may have resulted in a reduced EP at the apex of the cochlea.

The region of maximal TLS and TTS aligned with the location and extent of the buckled pillar cells (Fig. 1(a)). The TLS peak at 1 kHz aligned with the border between normal and buckled pillar cells. Curiously, the local peak at 4 kHz aligned with the apical edge of the focal loss of OHCs, but is in the opposite direction from that which would be expected. Moving the TLS and noise floor curves two points to the right (i.e., plotting the data at f_2) would place the local peak in the center of the lesion. However, the degree of alignment with the buckled pillar cells would be reduced if the data were plotted at f_2. The TLSs from the other four L_1, L_2 combinations are shown in Fig. 1(b). Their patterns were similar in some ways, particularly at the focal lesion (vertical gray bar), and different in others, such as in the region of the boundary between normal and buckled pillar cells. The biggest difference overall was with the 75, 55 dB L_1, L_2 combination (stars).

3.2. Mean temporary level shift

The mean $2f_1-f_2$ DPOAE TLSs for the three exposures (80 dB SPL, circles; 86 dB SPL, squares; 92 dB SPL, diamonds) and five L_1, L_2 combinations (75, 65; 75, 55; 65, 65; 65, 55; and 55, 55) are shown in Figs. 2(a)–(e). The data from the right ear of 989 were not included in the means because of poor pattern correlations ($r=0.4$ to 0.6) compared to all the others in the 92 dB SPL group ($r=0.7$ to 0.96). The data have been plotted at f_1 for the reasons stated above. Error bars have been omitted for clarity, but the logarithmic

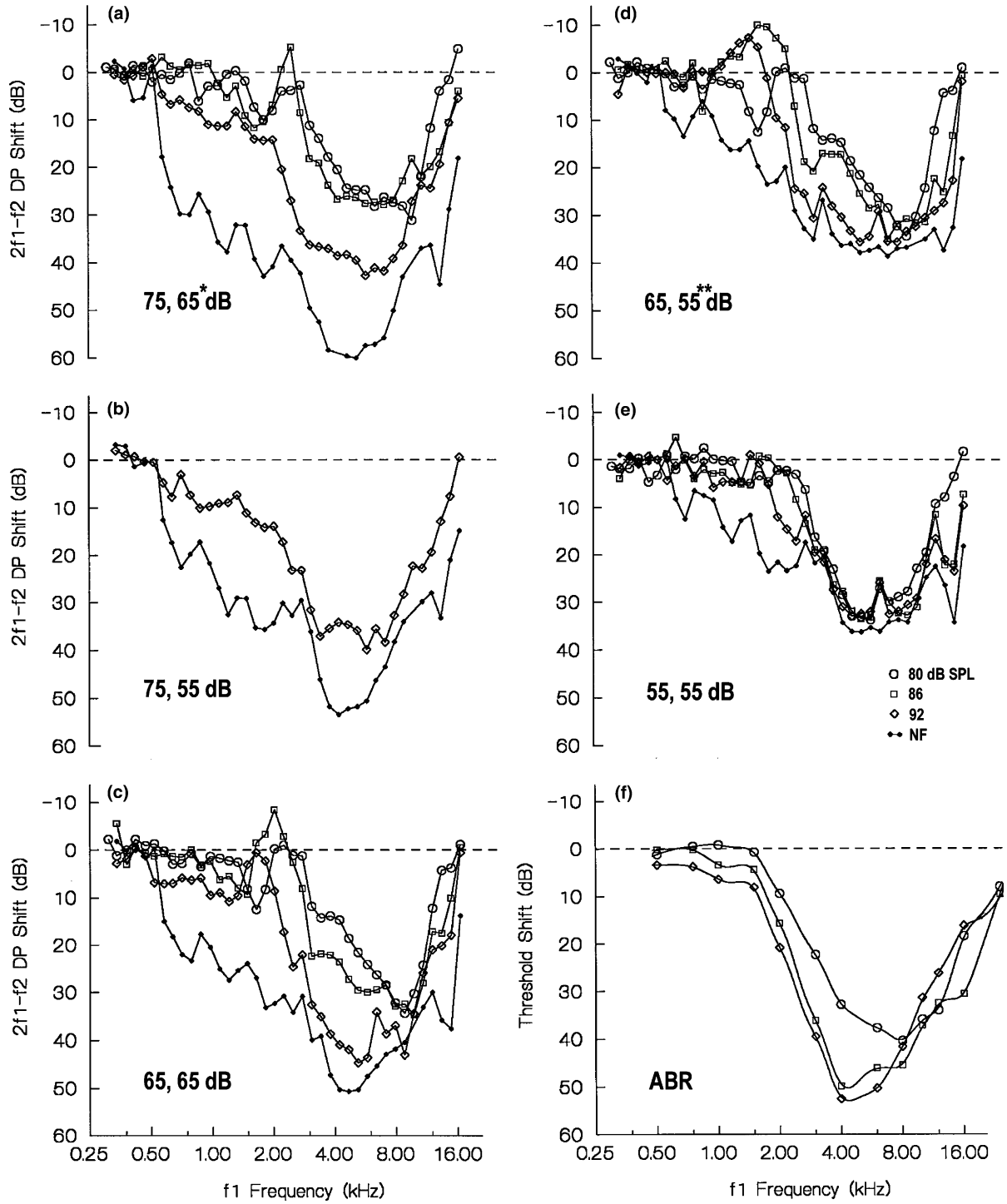

Fig. 2. (a–e) Mean DPOAE TLS for L_1, L_2 combinations shown and exposure SPLs (80 dB, circles; 86 dB squares; 92 dB, diamonds) and differential noise floor (NF; solid dots) plotted at frequency f_1. (f) Mean ABR TTS (same symbols as in a–e). Error bars omitted for clarity. (At 80 dB SPL: * L_1, $L_2=65$, 75; ** L_1, $L_2=55$, 65).

variances were similar to those shown in Table 2. In Fig. 2(a), the L_1, L_2 combination 75, 65 was not run in the 80 dB SPL animals, so the results at 75, 75 dB are shown. Similarly, the 65, 55 combination was not run in the 80 dB animals, so the results from 65, 65 dB from Fig. 2(c) are repeated in Fig. 2(d) for comparison.

In general, the TLS in the region from 2 to 12 kHz increased with increasing SPL of the exposure. The TLS was minimal from 0.3 to 1.5 kHz, gradually increased to a maximum from 2 to 12 kHz, and returned to baseline at 13–16 kHz. However, the patterns of shift were variable. Within the 2–12 kHz region, some TLSs were 'U' shaped and others were high-frequency (basally) skewed and 'V' shaped. For the most part, the maximum shift moved to a lower frequency (apically) as the SPL of the exposure was increased and the range of affected frequencies increased. In many instances, there appeared to be a 'W' shaped bimodal maximum (e.g., Fig. 2(c), 92 dB SPL, ~4 and 8 kHz). The frequency place of the valleys and intervening local peak was variable. In addition, there was almost always a leading, sometimes negative, local peak (e.g., Figs. 2(c) and (d), ~1.5–2 kHz) with a local valley apical to it.

The mean ABR TTS for the three exposures is shown in Fig. 2(f). In general, the magnitude from 2 to 16 kHz increased with increasing SPL of the exposure. The maximum shift was about 10 dB greater than for the corresponding TLS. Like the TLS, the maximum moved to a lower frequency and the affected frequency range widened as the SPL of the exposure increased. The TTS was wider than the TLS and each TLS fit neatly inside its corresponding TTS.

Because the subtle features of the TLS patterns showed variable frequency place, averaging the data across animals and ears would tend to reduce the magnitudes of these components. Therefore, a different approach was taken to analyze the components of the responses (see below).

3.3. Pattern measurements

Data were assembled from the individual DPOAE recordings at each level combination to characterize the magnitudes of the dominant features and the f_1 frequency place where they occurred. Fig. 3 illustrates (974R at L_1, L_2 = 55, 55 dB) how these data were collected. The magnitudes and frequency places of the departure from baseline (a), the bottom of the local valley (b), the maximum of the leading local peak (c), and the end of the leading local peak or the inflection point (d) were entered into the data set. The magnitudes of the three adjacent samples containing the local valleys (e and g) were averaged and the results and frequency place of the middle sample were determined. The magnitudes and frequency places of the intervening local peak (f) and the return to baseline (h) were also determined. The logarithmic mean magnitude and harmonic mean frequency-place were then computed for each exposure SPL and L_1, L_2 combination. In three out of the 108 cases (964L at 65, 65; 965L at 55, 55; and 991R at 75, 55), the magnitude at point c minus that at point b (amplitude of leading local peak) was less than 3 dB. This was considered to be within the margin of error and these points were excluded from the calculation for the magnitude at point c. The magnitude of the differential noise floor at the sampling points (a–h) was not entered.

The results from these calculations are shown in Fig. 4 for the individual L_1, L_2 combinations. The L_1, L_2 combinations are arranged somewhat differently than in Fig. 2 in order to accommodate the results at 75, 75 from animal 960 which was run at slightly different frequencies than the others. In each panel, distance-weighted least-squares was used to calculate smooth curves through the mean magnitude by mean frequency points for the available data at each of the three exposure SPLs. The magnitudes at points a and h were arbitrarily set to zero to start and end the curves at baseline. The patterns can be seen more clearly here than in Fig. 2. Error bars have been omitted for clarity, but the logarithmic and harmonic variances are presented in Table 2.

In Fig. 4, the bimodal local valleys (i.e., e and g in Fig. 3) moved to a lower frequency with increasing SPL of the exposure. The intervening local peak (i.e., f in Fig. 3) was much more apparent than in Fig. 2 and moved apically with the local valley. The leading local peak (i.e., c in Fig. 3) was much more apparent and moved to a lower frequency with increasing SPL of the exposure as well. However, there were some subtle differences with changes in exposure SPL. With the 80-dB exposure (circles), the magnitude of the first local valley (e) was less than the second (g), except at 65, 55 and 55, 55 dB. The magnitude of the leading local peak (c) was more pronounced with the 86-dB exposure (squares) except for 75, 75 dB.

Fig. 5 shows the data plotted by exposure SPL so that the patterns from the L_1, L_2 combinations (75, 75 – circles; 75, 65 – squares; 75, 55 – triangles; 65, 65 – diamonds; 65, 55 – pentagons; 55, 55 – stars) can be compared. In general, the magnitude of the TLS increased with increasing SPL of the exposure. The frequency places of the first and second local valleys (e and g) and the intervening local peak (f) moved around a bit, but generally not in a consistent way relative to the overall magnitude of L_1 and L_2 (Table 2). The magnitude and frequency place of the leading local peak was variable and did not appear to be related to L_1 and L_2.

Table 2
Means and standard deviations for magnitude (P/P_0) and frequency place ($1/f_1$) of component measures shown in Fig. 3

L_1, L_2 (dB)	b[A]	c[A]	d[A]	e[A]	f[A]	g[A]
80 dB SPL						
75, 75	4.5[B]	1.2	3.6	16.5	15.6	30.6
	3.7[C]	0.5	0.7	10.7	10.3	16.4
	0.49[B]	0.39	0.33	0.20	0.18	0.12
	0.04[C]	0.03	0.01	0.03	0.03	0.01
65, 75	2.8	0.8	1.7	16.9	11.7	26.1
	1.9	0.3	0.3	12.1	4.6	3.4
	0.43	0.36	0.32	0.17	0.14	0.11
	0.04	0.01	0.00	0.00	0.02	0.00
65, 65	3.1	0.8	1.5	13.2	13.0	43.9
	2.0	0.2	0.7	7.2	8.5	16.6
	0.57	0.45	0.36	0.22	0.18	0.12
	0.11	0.05	0.02	0.04	0.02	0.01
55, 65	2.3	0.7	2.9	15.9	10.7	18.3
	1.1	0.0	0.0	6.4	2.0	3.7
	0.58	0.44	0.35	0.20	0.17	0.12
	0.12	0.09	0.08	0.01	0.04	0.01
55, 55	2.3	1.0	1.8	41.1	17.8	38.4
	0.1	0.2	0.6	16.7	8.9	25.1
	0.56	0.41	0.37	0.22	0.18	0.14
	0.14	0.05	0.03	0.03	0.04	0.03
86 dB SPL						
75, 75	4.2	2.4	4.1	48.6	56.9	69.5
	0.4	0.4	0.4	11.7	37.2	32.2
	0.56	0.50	0.40	0.26	0.22	0.14
	0.00	0.00	0.00	0.01	0.05	0.00
75, 65	4.6	0.4	2.2	19.5	15.0	27.9
	3.3	0.3	1.3	5.1	8.4	4.9
	0.59	0.43	0.35	0.21	0.18	0.13
	0.05	0.04	0.03	0.05	0.06	0.05
65, 65	3.5	0.3	2.2	24.9	19.5	56.5
	1.7	0.1	0.7	8.6	2.9	25.0
	0.72	0.54	0.35	0.20	0.18	0.13
	0.06	0.07	0.03	0.05	0.05	0.03
65, 55	1.1	0.2	1.2	24.6	19.2	47.2
	0.8	0.1	0.5	16.6	12.5	13.4
	0.83	0.59	0.41	0.20	0.17	0.13
	0.15	0.06	0.06	0.08	0.07	0.03
55, 55	2.3	0.8	1.8	52.1	18.3	42.4
	1.1	0.2	0.7	17.1	6.2	20.7
	0.74	0.55	0.43	0.19	0.15	0.12
	0.08	0.11	0.06	0.00	0.01	0.01
92 dB SPL						
75, 65	6.7	1.7	5.6	73.6	52.7	136.5
	4.7	1.0	3.8	53.1	41.7	88.1
	0.68	0.53	0.45	0.30	0.24	0.16
	0.19	0.13	0.11	0.03	0.04	0.02
75, 55	4.7	1.5	4.5	61.4	42.2	82.0
	1.6	1.0	1.9	35.9	22.5	44.1
	0.78	0.60	0.50	0.28	0.23	0.16
	0.27	0.16	0.12	0.02	0.04	0.02
65, 65	5.1	0.6	1.9	110.9	38.4	109.2
	3.1	0.4	0.6	84.7	19.3	58.1
	0.82	0.59	0.47	0.24	0.20	0.15
	0.12	0.07	0.06	0.05	0.07	0.04
65, 55	1.8	0.3	1.6	47.2	15.8	59.8
	2.2	0.1	0.8	27.1	9.2	16.9
	1.00	0.71	0.50	0.25	0.19	0.14
	0.25	0.14	0.07	0.06	0.05	0.03
55, 55	3.9	0.7	3.1	43.0	13.3	41.3

Table 2 (*continued*)

L_1, L_2 (dB)	b[A]	c[A]	d[A]	e[A]	f[A]	g[A]
	4.9	0.5	2.6	19.4	8.7	13.8
	0.68	0.57	0.45	0.23	0.19	0.13
	0.16	0.15	0.10	0.08	0.08	0.02

[A] Sampling points from Fig. 3.
[B] Means and [C]standard deviations of P/P_0 (above) and $1/f_1$ (below).

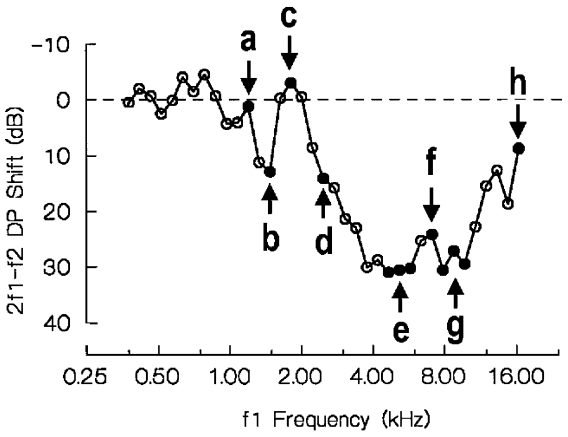

Fig. 3. TLS pattern measurement points (a–h; filled circles) for magnitudes and frequency place f_1 in cochlea 974R at $L_1 = L_2 = 55$ dB. Three adjacent points at e and g averaged.

3.4. Recovery from temporary level shift

Fig. 6 shows the TLS (open circles) and TTS (solid circles) for 989L at 0 days of recovery and the cytocochleogram, DPOAE level shift (open squares) and ABR threshold shift (solid squares) at 7 days of recovery. OHC and IHC losses were minimal except in the 6–12 kHz region, a distance of 2 mm (Fig. 6(a)). There was a 0.24-mm lesion of 100% OHC loss at 12 kHz. Apical to this lesion was a region (6–12 kHz) with 20% OHC loss where most of the remaining OHCs were distorted and swollen. From 1 to 6 kHz, the OHCs were out-of-position and slightly shrunken. The bodies of the pillar cells had partially recovered from 2 to 6 kHz, but were still not parallel to one another. From 6 to 12 kHz, the pillar cells were buckled.

The TLSs (Fig. 6(a), open circles; Fig. 6(b)) and TTS (Fig. 6(a); solid circles) were part of the analysis in Fig. 4 and thus, similar to the data presented. The level shift at 7 days did not change much between 0.4 and 1.5 kHz (Figs. 6(a) and (c)). The level shift in the 2–12 kHz region greatly improved, but the residual level shift still coincided with the extent of injured pillar cells. There was a region of partial DPOAE recovery (Fig. 6(a)), which coincided with the focal lesion and adjacent, severe pathological changes in the OHCs. With other L_1, L_2 combinations (Fig. 6(c)), the recovery in the same region (vertical gray bar) was similar but varied somewhat above and below the focal lesion. All combinations showed moderate recovery in the region of OHC damage and loss; many with a region where the TLS was in the opposite direction from what would be expected.

In all of the ears which were allowed to recover, the magnitude of the DPOAE level shift in the 2–12 kHz region diminished with time. The TLS and TTS in all six of the ears exposed at 80 dB recovered completely by 2 days, except for the TTS in 963L at the focal lesion. Only two of the four ears exposed at 86 dB and allowed to recover showed complete DPOAE recovery by 10–14 days; the other two had only partial recovery by 21–24 days. The TTS had not completely recovered in any of these ears. None of the four ears exposed at 92 dB and allowed to recover showed complete TLS and TTS recovery by 7 or 14 days. Over recovery time, the magnitude of the leading local peak (c in Fig. 3) decreased and its frequency place moved basally to a higher frequency. In those ears which showed complete DPOAE recovery, the leading local peak disappeared altogether.

As shown in Harding et al. (2002) (Fig. 4(b)), the DPOAEs in ear 963L (80-dB exposure) with an equal L_1 and L_2 of 75, 65 and 55 dB had completely recovered by 13 days, including at a focal lesion. These TLS patterns were similar to those shown here and the TTS was the same. The ABR threshold shift at 13 days of recovery showed a notch which aligned with the 0.4-mm near wipeout that involved loss of all IHCs, OHCs, inner and outer pillar cells and many Deiters' cells. In addition, 85% of the nerve fibers to the lesioned area were missing. Unequal levels with $L_2 = L_1 + 10$ dB were done in animal 963, but the data were not processed until recently. Surprisingly, the DPOAE level shift in the left ear from the 55, 65 combination for L_1 and L_2 at 13 days of recovery showed a narrow local valley or notch at 6 kHz which was aligned with the OHC loss in the lesion (Fig. 7; open squares at 6 kHz). A notch in the ABR threshold shift at the same location and recovery time (Fig. 7; solid squares at 6 kHz) also occurred as a consequence of the IHC and nerve fiber loss in the lesion. Interestingly, the level-shift notch was already evident at 6 and 9 days of recovery with the $L_2 = L_1 + 10$ dB combinations.

3.5. Focal lesions

Focal lesions involving OHCs occurred in one of the six cochleae exposed at 80 dB SPL (963L, 13-day

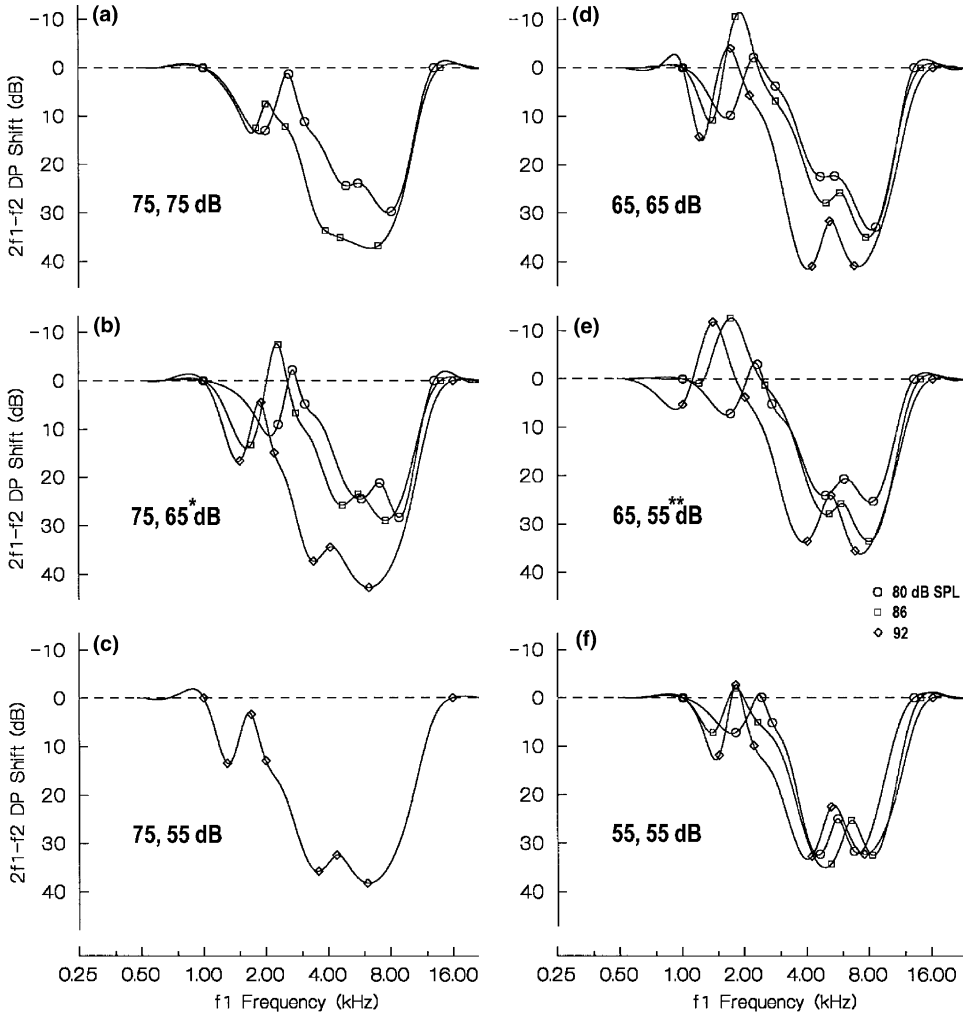

Fig. 4. (a–f) Mean TLS magnitude and frequency place f_1 patterns for L_1, L_2 combinations shown and exposure SPL (80 dB, circles; 86 dB, squares, 92 dB diamonds). (a,c) All exposure SPLs were not run at each L_1, L_2 combination. (At 80 dB SPL: * L_1, L_2=65, 75; ** L_1, L_2=55, 65).

recovery), three of the eight cochleae exposed at 86 dB SPL (960L at 24 days; 967R at 10 days; and 974R at 0 days), and 11 of the 12 cochleae exposed at 92 dB SPL (985L and R, 986L and R, 987L and R, 988L and R, 989L and R, 991L, 0–14 day recovery). All but the lesion in 986R were smaller (0.1–0.7 mm) than the one shown in Fig. 1 and their frequency place was variable (Table 3). At 0 days of recovery, only 15 of the 42 (36%) tested combinations in cochleae with focal lesions had a narrow, aligned local valley (notch), 14 (33%) combinations resulted in a narrow local peak (enhancement), while 13 (31%) combinations had neither a notch nor an enhancement. When plotting the data at f_2 rather than f_1, 10 (24%) combinations revealed a notch, 21 (50%) combinations showed an enhancement, while 11 (26%) combinations showed neither (Table 3). The frequency-place of an enhancement and focal lesion was often at the intervening local peak.

With 7–24 days of recovery, 12 of the 23 (52%) tested combinations had an aligned notch at a focal lesion, 7 (30%) produced an enhancement, and 4 (17%) showed neither. Plotting the data at f_2, 15 (65%) showed a notch, 4 (17.5%) an enhancement, and 4 (17.5%) neither. After recovery, there was a slightly higher likelihood that the correspondence of a notch with a focal lesion was better when the data were plotted at f_2 rather than at f_1. However, there was little consistency among the L_1, L_2 combinations which produced a notch, an enhancement or neither in the two ears of the same animal or across animals. In cochleae without a focal lesion, 1 of the 12 combinations at 0 days and 10 of the 31 after 6–21 days of recovery showed a notch in the region where focal lesions would be expected to occur, a 32% false positive rate with the levels used here.

3.6. f_2-f_1 DPOAE level shift

It was shown in Harding et al. (2002) (Fig. 7(a)) that f_2-f_1 had a local valley that coincided with the 0.4-mm focal lesion at 6 kHz in 963L (Fig. 7). The f_2-f_1

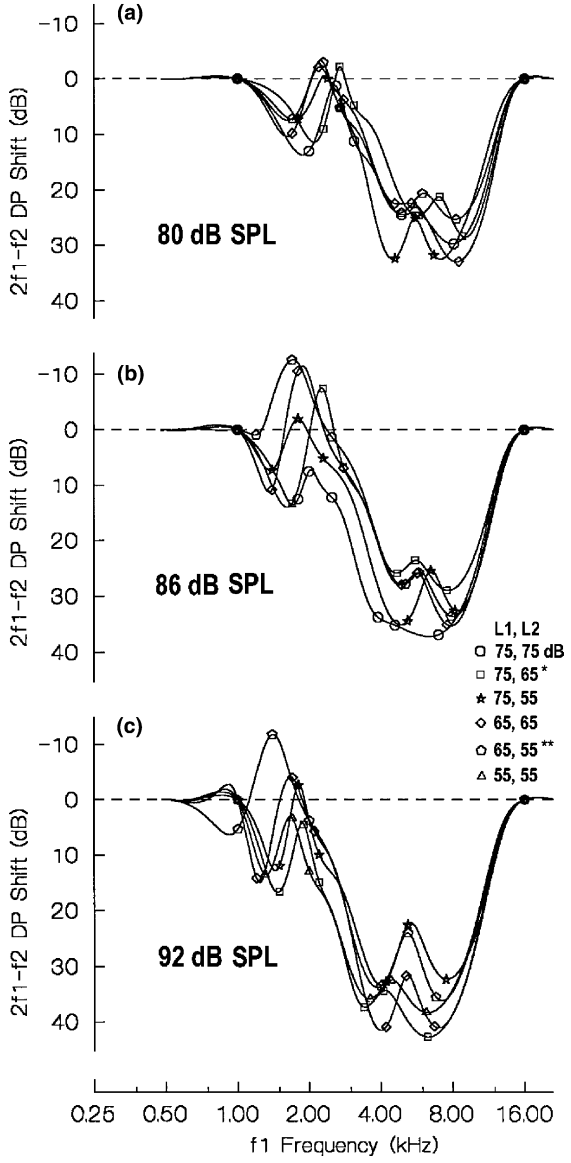

Fig. 5. (a–c) Mean TLS magnitude and frequency place (f_1) patterns for exposure SPLs shown and L_1, L_2 combinations (L_1, L_2 = 75, 75, circles; 75, 65, squares; 75, 55, stars; 65, 65, diamonds; 65, 55, pentagons; 55, 55, triangles). All L_1, L_2 combinations were not run at each exposure SPL. (At 80 dB SPL: * L_1, L_2 = 65, 75; ** L_1, L_2 = 55, 65).

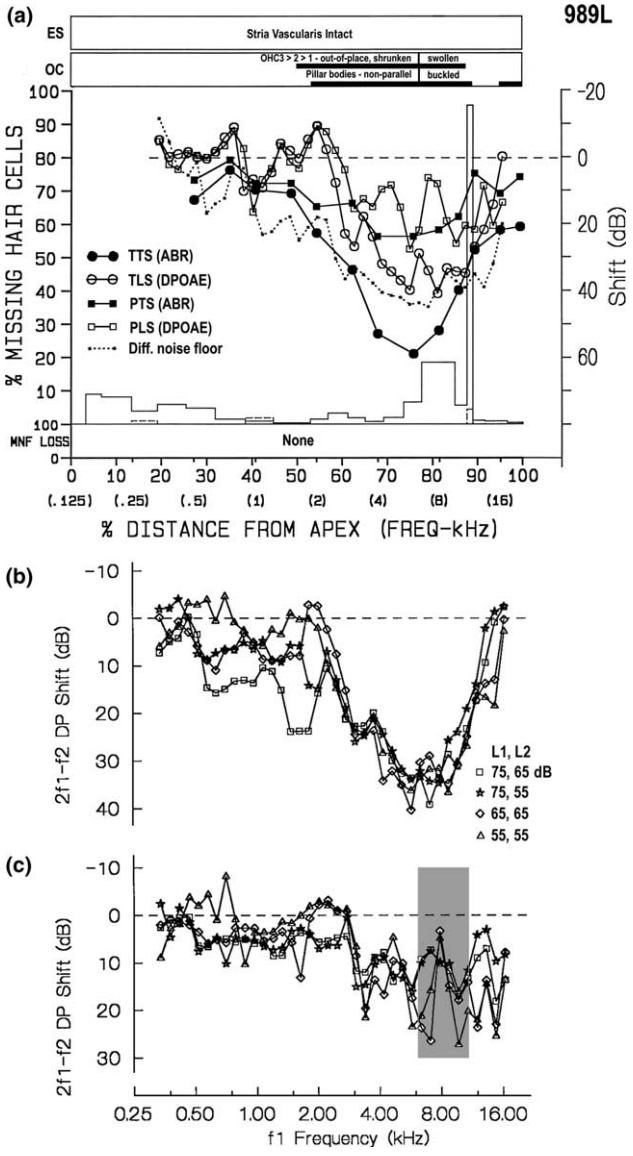

Fig. 6. (a) Cytocochleogram and functional data for cochlea 989L (exposed at 92 dB SPL). TLS data (symbols as in Fig. 1), and level (open squares) and threshold (filled squares) shift at 7 days of recovery are shown. There is a focal lesion at 12 kHz and 20% OHC loss from 6 to 12 kHz. At 7 days of recovery, pillar cell bodies were not parallel to one another from 1.5 to 6 kHz and remained buckled from 6 to 10 kHz (OC box; lower horizontal bars). OHCs were out-of-place, shrunken, or swollen from 1 to 9 kHz (OC box; upper horizontal bars). The stria vascularis was intact (ES box). (b) TLS data for L_1, L_2 combinations not shown in (a) (symbols as in Fig. 1). (c) Level shifts at 7 days of recovery for L_1, L_2 combinations not shown in (a) (symbols as in Fig. 1). Region of OHC loss or severely impaired function indicated by vertical gray bar. Level shift y scale in (a) differs from (b) and (c). Error bars omitted for clarity.

DPOAE was examined in the ears other than 963L with focal lesions greater than or equal to 0.7 mm in length (the approximate distance on the chinchilla basilar membrane between the frequency places of f_1 and f_2). It was found that f_2-f_1 DPOAEs at some L_1, L_2 combinations showed a substantial notch at a focal lesion of similar size. However, other L_1, L_2 combinations, even in the same ear, did not. An example is shown in Fig. 8 for ear 989L, the same ear in Fig. 6 for $2f_1-f_2$ DPOAE shift. Although the f_2-f_1 DPOAEs had a smaller magnitude than the $2f_1-f_2$ DPOAEs, the TLS patterns from 2 to 12 kHz (Fig. 8(a)) were indistinguishable. At 7 days of recovery (Fig. 8(b)), the 75, 55 and 65, 55 combinations showed a distinct local valley which aligned with the lesion. However, the other combinations had a local peak at this location, much like those from $2f_1-f_2$. The f_2-f_1 patterns of TLS in animals 986 and 988 at 0 days of recovery were also indistinguishable from those at $2f_1-f_2$ in the 2–12 kHz region.

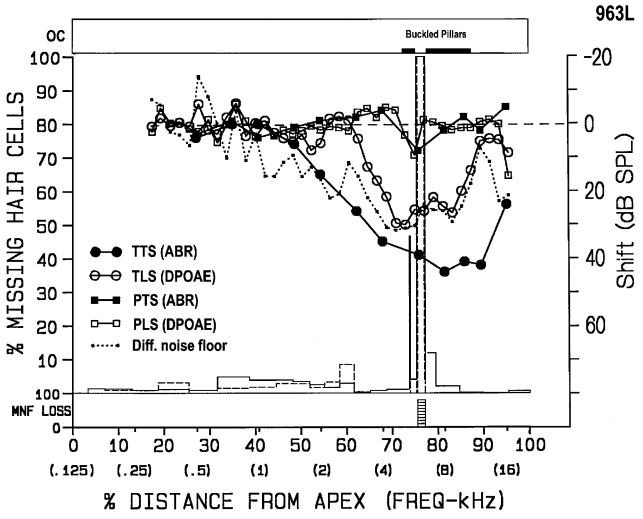

Fig. 7. Cytocochleogram and functional data immediately post-exposure and at 13 days of recovery for cochlea 963L (exposed at 80 dB SPL; $L_1 = 55$, $L_2 = 65$ dB; symbols same as in Fig. 6a). Both the level shift (open squares) and threshold shift (filled squares) at 13 days of recovery show a notch at 6 kHz which coincided with the focal OC lesion, nerve fiber loss (MNF LOSS box at bottom) and buckled pillar cells (OC box; horizontal bars). The stria vascularis was intact (ES box). (After Harding et al., 2002; Fig. 4b).

In animal 986 at 7 days of recovery, $f_2 - f_1$ DPOAE level shifts with all L_1, L_2 combinations were much like the patterns from $2f_1 - f_2$ in this region.

4. Discussion

The data from the 92-dB exposures provide an answer to the question raised in Harding and Bohne (2004) regarding 'critical level' in chinchillas. In that report, critical level for OHC loss was thought to be about 90 dB. However, there were no animals included which were exposed to a 4-kHz OBN between 86 and 108 dB. The 86-dB exposure was clearly below critical level and the 108-dB exposure was well above it. Here, the 92-dB exposures produced OHC loss which was at the margin between below versus above critical level as defined in Harding and Bohne (2004). Thus, the cochleae in the present study did not sustain OHC loss by both primary and secondary mechanisms (i.e., loss occurring during versus after the exposure) whereas the 108-dB exposed cochleae reported in Harding et al. (2002) probably did.

The frequency range of both the TLS and TTS aligned with the extent of injured supporting cells, especially buckled pillar cells. As the SPL of the exposure was increased, pillar buckling extended further apically and the magnitudes of the shifts increased. It has been shown that this buckling is associated with a reduction in the height of the OC (Harding et al., 1992) and an uncoupling of the OHC stereocilia from the tectorial membrane (Nordmann et al., 2000). We hypothesize that OC height reduction would also disconnect the IHC stereocilia from their contact with Hensen's stripe. The magnitude of the functional shifts would depend on the degree of supporting-cell damage. As the SPL and/or duration of the exposure is increased, the supporting cells would collapse further and further, resulting in less and less energy being transmitted from the basilar membrane to the reticular lamina.

The patterns of TLS in chinchillas were similar to level shifts seen in rabbits 4–5 weeks after a 6-h exposure to a 105-dB OBN centered at 2 kHz (Howard et al., 2003). In rabbits, the leading local peak, first local valley, and a hint of the intervening local peak were also similar when a 5.962 kHz, 75 dB interference tone was introduced (Martin et al., 1987). A similar level-shift pattern was also seen in the guinea pig soon after

Table 3
Ear, recovery time and focal lesion size and frequency-place

Ear	Recovery time (days)	Focal lesion (mm)	f_1 @ center (kHz)	Notch @ f_1[a] (L_1, L_2; dB)	Enhancement @ f_1[a] (L_1, L_2; dB)
974R	0	0.36	6.7	65, 55	65, 65
985L	0	0.24	7.9	65, 55; 55, 55;	–
985R	0	0.27	8.2	55, 55	65, 6 5
987L	0	0.09	7.3	65, 65	75, 65; 65, 55; 55, 55
987R	0	0.21	6.2	75, 65	65, 65; 65, 55; 55, 55
988L	0	1.06	5.0	65, 65; 55, 55	75, 65; 75, 55
988R	0	0.69	4.3	55, 55	75, 65; 75, 55; 65, 65; 65, 55
991L	0	0.22	10.0	75, 65; 75, 55; 65, 55	–
991R	0	0.23	13.0	75, 65; 65, 55; 55, 55	–
989L	7	0.24 (+1.82)[b]	11.0 (8.0)[b]	75, 65; 75, 55; 65, 65; 65, 55; 55, 55	–
960L	10	0.12 (+1.18)[b]	7.7 (8.6)[b]	–	–
963L	13	0.38	6.0	55, 65; 55, 55	65, 75
986L	14	0.70	4.0	65, 65	75, 65; 65, 55; 55, 55
986R	14	1.16 (+1.68)[b]	6.0 (4.0)[b]	65, 65; 55, 55	75, 65; 65, 55
967R	24	0.24	11.0	65, 55; 55, 55	75, 65

[a] L_1, L_2 combinations not listed showed neither a notch nor an enhancement.
[b] Region with 20% OHC loss and the remainder damaged.

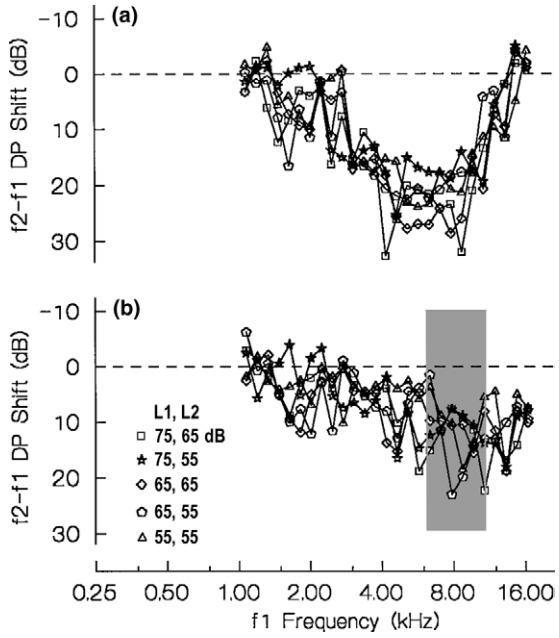

Fig. 8. (a) TLS for f_2-f_1 in cochlea 989L immediately post exposure (same cochlea as in Fig. 6). (b) Level shift for f_2-f_1 at 13 days of recovery. Symbols same as in Fig. 6(b) and (c). Region of OHC loss or severe impairment indicated by vertical gray bar.

exposure to a 110 dB, 2.176 kHz tone for 45 min (Cianfrone et al., 1998). Chang and Norton (1996) exposed guinea pigs to a half OBN centered at 4, 6 or 8 kHz at either 80 or 90 dB SPL for 4 h. Chang and Norton's (1996) data (Fig. 1, single animals) were digitized in order to determine the pre- and post-exposure $2f_1-f_2$ DPOAEs ($L_1=65$, $L_2=55$ dB) for the three half OBNs

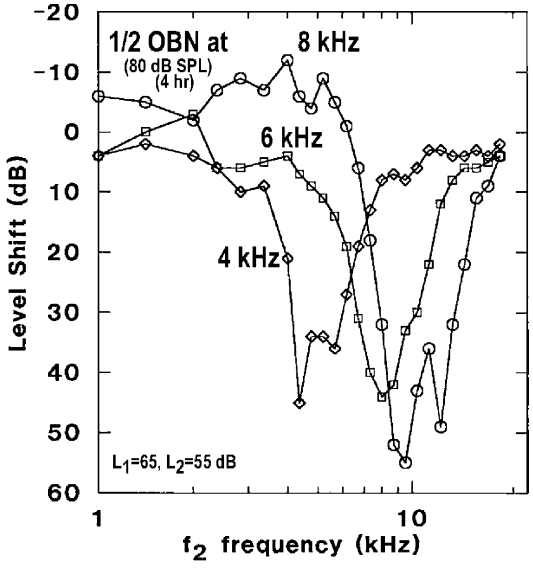

Fig. 9. TLS calculated from individual guinea pig data in Chang and Norton (1996; Fig. 1) for $2f_1-f_2$ DPOAEs, ($f_2/f_1=1.26$, $L_1=65$, $L_2=55$ dB) shortly after exposure to an 80 dB, half OBN centered at either 4 (diamonds), 6 (squares) or 8 kHz (circles).

at 80 dB. When the TLS was calculated (Fig. 9), the resulting patterns at 4 and 8 kHz were remarkably similar to those presented here. Thus, the patterns shown here are not unique to the chinchilla.

Both the maximal TLS and TTS moved to a lower frequency (i.e., apically) as the SPL of the exposure was increased. For the TLS, the frequency place of the leading and intervening local peaks moved apically with the maximal TLS. This movement contrasts with the observations that the maximally stimulated region by mid- or high-frequency tones or narrow bands moves basally as intensity is increased (Cody and Johnstone, 1981; Liberman and Mulroy, 1982; as cited by Wang et al., 2002). In addition, the group means for an 80 or 90 dB, half OBN centered at 6 kHz in Chang and Norton (1996) did not show an apical shift of the pattern components with increasing SPL of the exposure. This discrepancy may be the result of variability in the frequency place of pattern details that disappeared when data from individual animals were averaged. However, these movements are consistent with the observations that for tones of the same frequency, the location of maximal basilar membrane displacement (e.g., Rhode and Recio, 2000) and velocity (e.g., Ren and Nuttall, 2001) moves apically as SPL increases.

Although the frequency-place moved apically as SPL of the exposure was increased, the location of the intervening local peak was about a half octave above the center of the OBN. A similar half-octave shift was seen with the half OBN exposure in guinea pigs (Chang and Norton, 1996). These findings are consistent with the half-octave shift of maximum hearing loss from a 4-kHz OBN exposure (e.g., Carder and Miller, 1972; Liberman and Mulroy, 1982), as well as pure tones (e.g., Cody and Johnstone, 1981). In chinchillas, focal lesions commonly form in the first turn following exposure to either a 0.5- or a 4-kHz OBN (e.g., Bohne, 1976; Clark and Bohne, 1978; Bohne et al., 1987). It is puzzling, therefore, that after the noise exposures used here, DPOAEs appeared to be less affected a half octave above the center of the OBN than those apical and basal to this location.

The leading local peak often showed enhancement of TLS magnitude. The frequency-place of the local peak generally corresponded to the boundary between buckled pillar cells (located basally) and normal pillar cells (located apically). If the OHCs at the boundary were hyper- and/or tonically active, this phenomenon could be a partial explanation for the tinnitus commonly associated with TTS-producing exposures (i.e., exposures where thresholds return to pre-exposure levels within 48 h).

At each of the exposure SPLs, it was surprising that the frequency-place of the components in the TLS patterns moved around depending upon L_1, L_2 combination. There was little consistency in these movements with decreasing L_1, L_2 levels, regardless of whether they

were equal or unequal. The 1.23 f_2/f_1 ratio and range for L_1 and L_2 used here were close to optimal over the same ranges in maps of both the non-noise-exposed rabbit (Whitehead et al., 1992) and guinea pig (Lukashkin and Russell, 2001). It is not known whether the optimal ratio and the optimal levels change after noise exposure.

The observed variation in the magnitude and frequency-place of the leading and intervening local peaks suggests that their mechanism(s) are independent from uncoupling of the stereocilia from the tectorial membrane. Uncoupling produces a broad, U-shaped pattern and the leading and intervening local peaks appear to be subtracted from this. Whether or not the leading local peak shows an enhancement depends upon its magnitude relative to that due to uncoupling. The location of the intervening peak then makes the pattern thereafter look like a balanced or unbalanced W-shape depending upon magnitude and where the peak occurred.

The leading local peak could reflect a local change in the operating point of the nonlinear transfer function (e.g., Frank and Kössl, 1997; Lukashkin and Russell, 2001) or a change in the shape of the transfer function or a combination of both. What would cause the operating point and/or the transfer function to change is unknown. It is likely that the underlying mechanism of these changes is intrinsic to the OC–basilar–membrane complex. However, this phenomenon could also be explained by a local increase in OHC sensitivity. The intervening local peak appears to reflect such an increase. The mechanism of this increase might be intrinsic to the OC as well. The sensitivity of OHCs at one location could also be modulated by the efferent system (Rajan, 2001) in response to the effects of the noise exposure on the local and adjacent regions of the OC. Raveh et al. (1998) found increased otoacoustic emissions adjacent to thermally induced lesions in the apical and middle turns of the chinchilla cochlea, regions where the OC was normal. It is interesting that in the present study, the frequency place of the leading and intervening local peaks was in the neighborhood of the apical and basal edges of the OBN, respectively. There is considerable evidence that experimental manipulation of the efferent system to the OHCs (e.g., electrical stimulation and noise in the contralateral ear) reduces CAP and DPOAE magnitudes (e.g., Puria et al., 1996). However, contrary to what would be expected after exposure of chinchillas to a broadband noise, cutting the efferent pathway to the OHCs reduced cochlear microphonic and DPOAE magnitudes as well (e.g., Zheng et al., 1997). On the other hand, Zheng et al. (2000) found in non-noise-exposed chinchillas that DPOAEs elicited with higher level primaries (such as those used in the present study) and lower frequencies (i.e., 1 and 2 kHz) were enhanced by 5–20 dB.

It has been shown that notches in the ABR threshold shift occur at focal lesions only if that lesion involves focal loss of IHCs (e.g., Nordmann et al., 2000). It was our expectation that with relatively large focal lesions (0.4–2.0 mm) involving 100% loss of OHCs, level shifts would show a distinct notch, but not necessarily to the noise floor, which would align with the lesion. However, the present results contradicted this expectation. Over all recovery times, only 42% of the tested combinations run on ears with focal lesions showed an aligned notch, 32% went in the opposite (enhanced) direction, and 26% showed neither a notch nor an enhancement. Although the magnitude of hair-cell loss in the two ears of the same animal has been shown to be highly correlated (Bohne et al., 1986), the present study showed little consistency in L_1, L_2 combinations which did or did not produce a notch or an enhancement in the two ears of the same animal or between animals receiving the same exposure. In a large study of chinchillas exposed to a variety of noises, Davis et al. (2004) found that the variability in post-exposure DPOAEs made it difficult to predict PTS or OHC loss. Whether or not other f_2/f_1 ratios and/or lower input level combinations would detect these lesions is unknown. On the other hand, for OHC lesions greater than 0.4 mm and over a range of input levels that are reasonably close to optimal, the f_2/f_1 ratio and/or the L_1, L_2 combination should not matter.

In a personal communication (2004), Glen K. Martin pointed out that the damage to supporting cells could explain why DPOAEs do not reliably detect focal lesions. The cochlea is not operating normally and DPOAEs are generated over a much broader region. For example, in 989L, DPOAEs that are expected to 'detect' the focal lesion must be generated in the presence of a very large region of abnormality consisting of buckled pillars and shrunken or swollen OHCs. Frequency selectivity is probably very poor and the overlap of the f_1 and f_2 primaries may be affected by this damage, allowing DPOAEs to be produced over a much broader region than when the OC is normal.

As reported in Harding et al. (2002), the best alignment of TLS with large regions of severe cell loss required plotting the data at f_1. It was also reported that partial or complete recovery of level shifts occurred at focal lesions involving 100% loss of hair cells and supporting cells. Most of these focal lesions were located at the frequency place of the intervening local peak. It was argued in Harding et al. (2002) that this paradox could be explained by difference tones coming from someplace other than $2f_1$, f_2 intermodulation (e.g., Fahey et al., 2000). This interpretation is probably valid for the results from the high-level (108 dB) exposures. However, it is unlikely that the results presented here can be explained on this basis; not just for focal lesions, but the leading and intervening local peaks as well. The apical half and basal 10% of the OC

in these animals was intact at 0 days. If distortion products were coming from someplace else, the components of the response should not move their frequency place apically if only the SPL of the exposure is increased.

As in the individual guinea pigs and group means of those exposed at 80 dB shown in Chang and Norton (1996), post-exposure DPOAE levels in the 80 dB exposed chinchillas had returned to pre-exposure levels after 2 days of recovery. Chang and Norton's guinea pigs exposed at 90 dB had only partially recovered by 8 days. Similarly, our chinchillas exposed at 86 and 92 dB had not completely recovered from their TLS by 10–24 days. If all OHCs are missing over a large region of the OC, the reticular lamina would be uncoupled from the tectorial membrane in that region. Even if nearly all IHCs are present and functionally normal, the loss of adjacent OHCs should disconnect the IHC stereocilia from Hensen's stripe and result in a permanent hearing loss and permanent reduction in DPOAEs.

It is surprising that $2f_1-f_2$ DPOAEs appear to be very sensitive to the condition of the supporting cells and the relation of these cells to stereocilia function and relatively insensitive to focal OHC loss. Although histopathological damage was not assessed by Chang and Norton (1996), they found that after noise exposure in guinea pigs, f_2-f_1 and $3f_1-2f_2$ DPOAEs appeared to be more sensitive than $2f_1-f_2$ DPOAEs. In chinchillas, the results from f_2-f_1 DPOAEs were similar to those from $2f_1-f_2$.

The clinical and screening use of DPOAEs to measure OHC status is an important issue. In cases of congenital hearing loss where DPOAEs are greatly reduced or absent, the status of OHCs in the end organ is clear. However, the implications from the present study suggest that commonly used DPOAE paradigms are not very reliable for detection of beginning (focal) loss of OHCs from noise damage. Thus, the use of DPOAEs to screen industrial workers for noise induced hearing loss may often miss the opportunity for early intervention and treatment.

5. Conclusions

1. The best correlation of DPOAE level shift with noise-induced histopathology from lower level, longer duration exposures occurred when these data were plotted at f_1.
2. Damaged supporting cells, especially buckled pillar cells, correlated well with the location and extent of the TLS and TTS.
3. The peak TLS and TTS and other components of the TLS response moved apically as the SPL of the exposure was increased.
4. $2f_1-f_2$ DPOAEs did not reliably detect relatively large focal lesions involving 100% OHC loss.
5. There was little consistency in L_1, L_2 combinations which did or did not produce a notch or an enhancement at focal lesions within the two ears of the same animal or between animals.
6. f_2-f_1 TLS patterns were similar to those at $2f_1-f_2$.

Acknowledgements

This work was supported by a Grant from NIOSH (OH 03973), an NIDCD training Grant (DC00071), and the Department of Otolaryngology, Washington University School of Medicine. The contents of this article are solely the responsibility of the authors and do not necessarily represent the official views of NIOSH. The authors are grateful for the contributions to the histopathological analyses by Steven Lee, Nicole C. Schmitt and Dr. Kenneth Hsu.

References

Ahmad, M., Bohne, B.A., Harding, G.W., 2002. An in vivo tracer study of noise-induced damage to the reticular lamina. Hear. Res. 175, 82–100.

Avan, P., Bonfils, P., Gilain, L., Mom, T., 2003. Physiological significance of distortion-product otoacoustic emissions at $2f_1$–f_2 produced by high- versus low-level stimuli. J. Acoust. Soc. Am. 113, 430–441.

Bohne, B.A., 1976. Safe level for noise exposure?. Ann. Otol. Rhinol. Laryngol. 85, 711–724.

Bohne, B.A., Harding, G.W., 1993. Combined organ of Corti/modiolus technique for preparing mammalian cochleas for quantitative microscopy. Hear. Res. 71, 114–124.

Bohne, B.A., Harding, G.W., 2000. Degeneration in the cochlea after noise damage: primary versus secondary events. Am. J. Otol. 21, 502–509.

Bohne, B.A., Bozzay, D.G., Harding, G.W., 1986. Interaural correlation in normal and traumatized cochleas: length and sensory cell loss. J. Acoust. Soc. Am. 80, 1729–1736.

Bohne, B.A., Gruner, M.M., Harding, G.W., 1990. Morphological correlates of aging in the chinchilla cochlea. Hear. Res. 48, 79–92.

Bohne, B.A., Yohman, L., Gruner, M.M., 1987. Cochlear damage following interrupted exposure to high-frequency noise. Hear. Res. 29, 251–264.

Cody, A.R., Johnstone, B.M., 1981. Acoustic trauma: single neuron basis for the "half-octave shift". J. Acoust. Soc. Am. 70, 707–711.

Canlon, B., Fransson, A., 1995. Morphological and functional preservation of the outer hair cells from noise trauma by sound conditioning. Hear. Res. 84, 112–124.

Carder, H.M., Miller, J.D., 1972. Temporary threshold shifts from prolonged exposure to noise. J. Speech Hear. Res. 15, 603–623.

Chang, K.W., Norton, S.J., 1996. The effects of continuous versus interrupted noise exposures on distortion product otoacoustic emissions in guinea pigs. Hear. Res. 96, 1–12.

Cianfrone, G., Ingrosso, A., Altissimi, G., Ralli, G., Turchette, R., 1998. DPOAE modifications induced by pure tone overstimulation in guinea pigs. Scand. Audiol. Suppl. 48, 37–43.

Clark, W.W., Bohne, B.A., 1978. Animal model for the 4-kHz tonal dip. Ann. Otol. Rhinol. Laryngol. Suppl. 51, 1–16.

Davis, B., Qiu, W., Hamernik, R.P., 2004. The use of distortion product otoacoustic emissions in the estimation of hearing and sensory cell loss in noise-damaged cochleas. Hear. Res. 187, 12–24.

Eldredge, D.E., Miller, J.D., Bohne, B.A., 1981. A frequency-position map for the chinchilla cochlea. J. Acoust. Soc. Am. 69, 1091–1095.

Fahey, P.F., Stagner, B.B., Lonsbury-Martin, B.L., Martin, G.K., 2000. Nonlinear interactions that could explain distortion product interference response areas. J. Acoust. Soc. Am. 108, 1786–1802.

Frank, G., Kössl, M., 1997. Acoustical and electrical biasing of the cochlea partition. Effects on the acoustic two tone distortions f_2-f_1 and $2f_1-f_2$. Hear. Res. 113, 57–68.

Harding, G.W., Bohne, B.A., 2004. Noise-induced hair-cell loss and exposure energy: analysis of a large data set. J. Acoust. Soc. Am. 115, 2207–2220.

Harding, G.W., Baggot, P.J., Bohne, B.A., 1992. Height changes in the organ of Corti after noise exposure. Hear. Res. 63, 26–36.

Harding, G.W., Bohne, B.A., Ahmad, M., 2002. DPOAE level shifts and ABR threshold shifts compared to detailed analysis of histopathological damage from noise. Hear. Res. 174, 158–171.

Howard, M.A., Stagner, B.B., Foster, P.K., Lonsbury-Martin, B.L., Martin, G.K., 2003. Suppression tuning in noise-exposed rabbits. J. Acoust. Soc. Am. 114, 279–293.

Liberman, M.C., Mulroy, M.J., 1982. Acute and chronic effects of acoustic trauma: cochlear pathology and auditory nerve pathophysiology. In: Hamernik, R.P., Henderson, D., Salvi, R. (Eds.), New Perspectives on Noise-Induced Hearing Loss. Raven Press, New York, pp. 105–135.

Lukashkin, A.N., Russell, I.J., 2001. Origin of the bell-like dependence of the DPOAE amplitude on primary frequency ratio. J. Acoust. Soc. Am. 110, 3097–3106.

Martin, G.K., Candreia, C., Bohne, B.A., Harding, G.W., Stagner, B.B., Lonsbury-Martin, B.L., 2002. An augmented acoustic environment delays age-related hearing loss in C57BL/6J mice as revealed by DPOAEs and cochlear histopathology. Abst. Assoc. Res. Otolaryngol. 25, 69–70.

Martin, G.K., Lonsbury-Martin, B.L., Probst, R., Scheinin, S.A., Coats, A.C., 1987. Acoustic distortion products in rabbit ear canal: II. Sites of origin revealed by suppression contours and pure-tone exposures. Hear. Res. 28, 191–208.

Nordmann, A.S., Bohne, B.A., Harding, G.W., 2000. Histopathological differences between temporary and permanent threshold shift. Hear. Res. 139, 13–30.

Puria, S., Guinan, J.J., Liberman, M.C., 1996. Olivocochlear reflex assays: effects of contralateral sound on compound action potentials versus ear-canal distortion products. J. Acoust. Soc. Am. 99, 500–507.

Rajan, R., 2001. Cochlear outer-hair-cell efferents and complex-sound-induced hearing loss: protective and opposing effects. J. Neurophysiol. 86, 3073–3076.

Raveh, E., Mount, R.J., Harrison, R.V., 1998. Increased otoacoustic-emission amplitude secondary to cochlear lesions. J. Otolaryngol. 27, 354–360.

Ren, T., Nuttall, A.L., 2001. Basilar membrane vibration in the basal turn of the sensitive gerbil cochlea. Hear. Res. 151, 48–60.

Rhode, W.S., Recio, A., 2000. Study of mechanical motions in the basal region of the chinchilla cochlea. J. Acoust. Soc. Am. 107, 3317–3332.

Wang, Y., Hirose, K., Liberman, M.C., 2002. Dynamics of noise-induced cellular injury and repair in the mouse cochlea. J. Assoc. Res. Otolaryngol. 3, 248–268.

Whitehead, M.L., Lonsbury-Martin, B.L., Martin, G.K., 1992. Evidence for two discrete sources of $2f_1-f_2$ distortion-product otoacoustic emission in rabbit: I. Differential dependence on stimulus parameters. J. Acoust. Soc. Am. 91, 1587–1607.

Zheng, X.Y., Henderson, D., Hu, B.H., Ding, D.L., McFadden, S.L., 1997. The influence of the cochlear efferent system on chronic acoustic trauma. Hear. Res. 107, 147–159.

Zheng, X.Y., McFadden, S.L., Henderson, D., Ding, D.L., Burkard, R., 2000. Cochlear microphonic and otoacoustic emissions in chronically de-efferented chinchilla. Hear. Res. 143, 14–22.